Pectin hydrogels, aerogels, cryogels and xerogels: Influence of drying on structural and release properties

Sophie Groult, Sytze Buwalda, Tatiana Budtova

Submitted to the European Polymer Journal 27 September 2020

Revised 22nd December 2020

Pectin hydrogels, aerogels, cryogels and xerogels: influence of drying on structural and release properties

*Sophie Groult, Sytze Buwalda, Tatiana Budtova**

MINES ParisTech, PSL Research University, Center for Materials Forming (CEMEF), UMR CNRS 7635, CS 10207, 06904 Sophia Antipolis, France

*Corresponding author: Tatiana Budtova

Tatiana.budtova@mines-paristech.fr

Highlights

- Various drying methods of pectin hydrogels were tested
- Aerogels, cryogels and xerogels were obtained and characterized
- The kinetics of theophylline release were studied
- Crosslinking with calcium strongly modifies the release kinetics of aerogels

Abstract

Pectin is an appealing material for biomedical applications because of its biocompatibility, bioactivity, biodegradability as well as its gelling and stabilizing properties. In this work, porous pectin cryogels, aerogels and xerogels were prepared via freeze-drying, sc drying and evaporative drying at 60 °C under low vacuum, respectively, starting from the same pectin precursor, a hydrogel. The physico-chemical and structural properties of the porous pectin matrices were investigated and related to the preparation conditions. The release of the model hydrophilic respiratory drug theophylline from all pectin networks, including the hydrogel, was studied and related to the network morphology and erosion profiles. The Korsmeyer-Peppas and Peppas-Sahlin models were used to determine the main physical mechanisms controlling the release. The release of theophylline can be tuned via the mode of pectin crosslinking in the initial hydrogel as well as via the drying method, demonstrating the potential of porous pectin matrices for drug delivery purposes.

Keywords: pectin; freeze-drying; supercritical drying; morphology; density; drug release.

1. Introduction

Pectin is an anionic, water-soluble polysaccharide constituting the cell walls of most plants. It is usually extracted from various types of fruits via enzymatic or chemical methods [1]. Pectin is widely used in the food industry as thickener, gelling agent, emulsifier, texturizer or colloidal stabilizer. In addition, pectin has received considerable attention for use in biomedical applications because of its biodegradability, biocompatibility, bioactivity as well as its gelling and stabilizing abilities [2, 3]. Pectin is gastro-resistant, which can be useful in oral drug delivery. Various pectin biomaterials, different in properties and applications, have been reported for controlled drug delivery [4] and 3D scaffolds for regenerative medicine [5]. Each application requires a specific morphology, density, internal pores surface area as well as pore size distribution. It is thus important to understand morphology development during processing and correlate it with material final properties.

There are different ways to make porous materials, one of them being drying a polymer system to remove its solvent. It is well known that the conditions during drying of hydrogels greatly impact the properties of the resulting porous networks [6, 7]. Evaporative drying usually leads to collapse of pores due to high capillary stresses. The resulting materials often exhibit a high density and low porosity [7]; for simplicity we will call them xerogels. Freeze-drying and drying under supercritical conditions, leading to so-called cryogels and aerogels, respectively, better preserve the open pore structure of the starting hydrogel. However, the morphology of the porous materials obtained after lyophilisation or supercritical drying is very different, as shown, for example, for cellulose [7]. Freeze-drying leads to the formation of large pores and channels from several microns to several tens of microns due to the growth of ice crystals and their sublimation. During supercritical drying, no liquid/gas meniscus and hence no surface tension exist, resulting in a better preservation of the

fine network structure. This leads to materials with mesopores and small macropores as well as a high specific surface area of several hundreds of m^2/g.

A number of publications report on porous pectin materials, including cryogels [8, 9], xerogels [10, 11] and aerogels [12-15]. Several works report on using pectin aerogels as delivery matrices. For example, pectin aerogel beads were made via dropping/prilling technique and used as carriers of anti-inflammatory drugs and of antibiotics [12, 16]. Pectin and pectin-alginate aerogel microspheres were prepared via emulsion-gelation technique and used for the release of the anti-inflammatory drug ketoprofen [13]. The release of the poorly water-soluble drug nifedipine was studied from pectin aerogel monoliths [17]. To the best of our knowledge only one method of drying was used for the preparation of the pectin materials in each publication, which makes the establishment of correlations between the drying method and material properties difficult.

This work has two goals. One is to determine the influence of drying conditions on the morphology and structural properties of porous pectin materials starting from the same pectin precursor (hydrogel); cryogel, aerogel and xerogel were prepared. The second goal is to compare the kinetics of drug release from all these materials including hydrogel. To reach these goals, the structural and physico-chemical properties of pectin cryogels, xerogels and aerogels were investigated and compared. Furthermore, the release of the water-soluble model drug theophylline, which is used in therapy for respiratory diseases such as chronic obstructive pulmonary disease (COPD) and asthma, was analyzed and related to the network morphology and erosion profile of the different pectin matrices. Kinetics models were employed to investigate the physical mechanisms governing the release.

2. Experimental section

2.1 Materials

Citrus pectin with a degree of esterification of 35% (as specified by the provider) was kindly donated by Cargill. Calcium chloride ($CaCl_2$) was from Acros Organics. Ethanol, potassium dihydrogen phosphate (KH_2PO_4), potassium hydroxide (KOH), sodium hydroxide (NaOH) and hydrochloric acid (HCl, 32%) were from Fisher Scientific. Theophylline was from Sigma Aldrich. All products were used as received. Simulated gastric fluid (SGF) was prepared from HCl solution (0.1 N, pH 1.0) and simulated intestinal fluid (SIF) (pH 6.8) was made using NaOH at 11 mM (0.65 g/L) and KH_2PO_4 at 50 mM (6.8 g/L). Water was distillated.

2.2 Methods

2.2.1 Preparation of pectin networks

Pectin hydrogels. Pectin solutions were prepared by dissolution of pectin powder in distilled water at a concentration of 6 wt% at 65 °C under stirring at 400 rpm. After complete dissolution, the solution pH was adjusted to pH 2.0 by adding a small quantity of HCl. Pectin solutions were then poured into molds of 27.5 mm in diameter. The aspect ratio (diameter to thickness) was between 2.3 and 2.5. In some cases, $CaCl_2$ was added under stirring, with the molar ratio R of Ca^{2+} ions to pectin carboxyl groups set to 0.2. Pectin solutions were let at rest for 48 h at room temperature, resulting in pectin hydrogels.

Pectin cryogels. Pectin hydrogels were prepared as described above and immersed in liquid nitrogen for approximately 5 minutes. Once completely frozen, the samples were freeze-dried (Cryotec Cosmos 80) for 48 hours to obtain pectin cryogels.

Pectin aerogels. In order to perform drying with sc CO_2, water has to be replaced by a fluid which is miscible with CO_2; ethanol was used for this purpose, it is a pectin non-solvent. The exchange

was performed by placing pectin hydrogels, prepared as described above, in consecutive baths with decreasing water/ethanol (v/v) ratios (50/50, 25/75 and 0/100), followed by final extensive washing with pure ethanol. The pectin alcogels were then dried with sc CO_2 (see details on drying parameters in reference [14]).

Pectin xerogels. Pectin alcogels were prepared as described above and placed in oven at 60°C under vacuum for at least 4 days to obtain pectin xerogels.

2.2.2 Loading of theophylline

To obtain theophylline-loaded pectin hydrogels and cryogels, the drug was dissolved in the pectin aqueous solutions at 3.4 g/L prior to the gelation step (Figure 1a). To obtain theophylline-loaded pectin aerogels and xerogels (Figure 1b), pectin alcogels were immersed in an ethanolic theophylline solution (3.4 g/L) with a volume 25 to 30 times larger than the volume of the pectin sample. The theophylline solution was renewed after 48 h and samples were immersed for 7 days in total to ensure complete drug diffusion through the sample. This duration was selected by calculating the time needed for a theophylline molecule to diffuse through a gel disk with a half thickness of maximum of 5 mm. For theophylline-loaded pectin aerogels, the impregnation of theophylline via ethanol was done at the step just before sc drying to minimize theophylline loss. For pectin xerogels this loading of theophylline was used for comparison with aerogels.

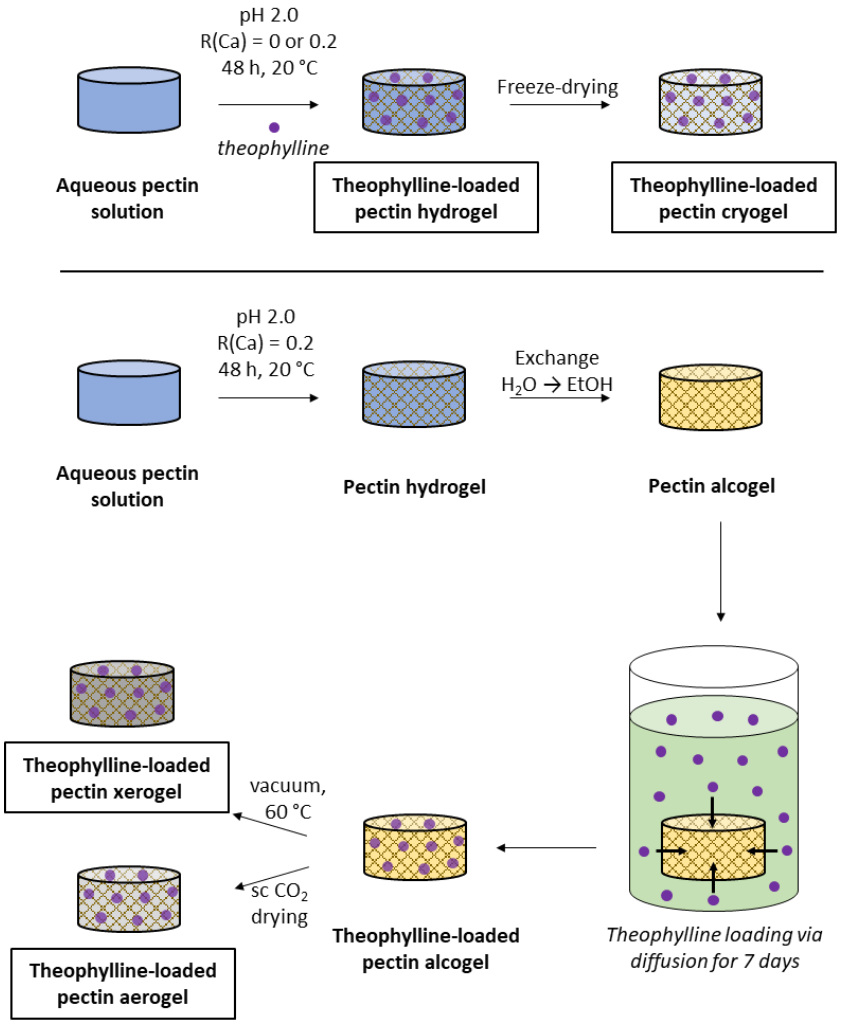

Figure 1.

Schematic illustration of the preparation of theophylline-loaded pectin hydrogels, cryogels, aerogels and xerogels.

2.2.3 Characterization methods

The bulk density of the pectin networks (ρ_{bulk}) was determined from the ratio of sample mass to sample volume. The mass and volume were measured with a high precision digital analytical balance and a digital caliper, respectively. Volume shrinkage due to solvent exchange and drying was determined as follows:

$$Volume\ shrinkage\ (\%) = \frac{V_h - V_d}{V_h} \times 100\% \quad (1)$$

where V_h and V_d are the volumes of the hydrogel before solvent exchange and of the dry network, respectively.

The porosity (ε) of the pectin networks, defined as the ratio between the volume of pores and the total volume of the sample, was estimated from the bulk and skeletal densities:

$$\varepsilon\ (\%) = \frac{V_{pores}}{V_{material}} \times 100\% = (1 - \frac{\rho_{bulk}}{\rho_{skeletal}}) \times 100\% \quad (2)$$

where the skeletal density of pectin networks ($\rho_{skeletal}$) is 1.5 g/cm^3 [14].

The specific pore volume (V_{pores}) was estimated also using the bulk and skeletal densities:

$$V_{pores} = \frac{1}{\rho_{bulk}} - \frac{1}{\rho_{skeletal}} \quad (3)$$

The specific surface area of the pectin networks (S_{BET}) was measured with a Micromeritics ASAP 2020 instrument using nitrogen adsorption and the Brunauer–Emmett–Teller (BET) method. The samples were degassed under high vacuum at 70 °C for 10 h prior to the measurements.

The morphology of the pectin networks was studied using a Zeiss Supra 40 scanning electron microscope (SEM) equipped with a field emission gun. A platinum layer of 7 nm was sputtered using a Q150T Quarum metallizer.

2.2.4 Theophylline release experiments

Theophylline release experiments were performed at 37 °C under sink conditions with stirring at 100 rpm to ensure homogenization. The pectin networks were placed in a permeable Inox basket which was immersed in SGF (pH 1.0) during 1 h and subsequently transferred to SIF (pH 6.8) to mimic the physiological conditions in the gastro-intestinal tract. Drug release was followed via

periodical spectrophotometric measurements at a wavelength of 271 nm using a quartz cuvette with an optical path length of 10 mm. An automated set-up was used, consisting of a UV-1800 UV/Visible Scanning Spectrophotometer coupled to a 206-23790-91 Peristaltic Sipper Pump and a 160C Sipper Unit (all from Shimadzu). If pectin was not completely dissolved after the release curve reached a stable absorbance plateau for more than 30 minutes, indicating that no more drug was released, the presence of theophylline in the remaining matrix was tested. The sample was crushed with a mortar and pestle and sonicated in SIF for 30 min. Subsequently a liquid probe was taken, filtered and its absorbance measured. In all cases no theophylline remained in non-dissolved matrices, and therefore the actual drug dose in the aerogel was the one of the released drug.

The drug loading efficiency and theoretical drug dose were calculated as follows:

$$Drug\ loading\ efficiency\ (\%) = \frac{actual\ drug\ concentration\ (g/cm^3)}{theoretical\ drug\ concentration\ (g/cm^3)} \times 100\% \qquad (4)$$

where the *Theoretical drug concentration* was calculated taking in account a slight dilution of theophylline in the loading bath due to the addition of pectin alcogel.

3. Results and Discussion

3.1 Characterization of drug-loaded pectin networks

Pectin cryogels, aerogels and xerogels were prepared via freeze-drying, sc drying and vacuum drying at 60 °C, respectively, using pectin hydrogels as a starting point (Figure 1). The gelation of pectin solutions depends on several conditions, including pectin concentration, pH and concentration of metal ions. At low pH, gelation occurs due to hydrogen bonds between hydroxyl and protonated carboxyl groups as well as hydrophobic interactions between methyl ester groups. The increase of solution pH to pectin pKa = 3 – 3.5 [18] results in carboxyl groups deprotonation;

in the presence of Ca^{2+} ions gelation takes place thanks to the formation of intermolecular junction zones via ionic bonds between Ca^{2+} ions and COO^- groups following the 'egg-box' model [18]. Here we will consider two cases: first, the influence of the drying method on the structural and physical properties of the pectin crosslinked with Ca^{2+} will be studied; theophylline loading efficiency and release kinetics will be analyzed as well. Based on our previous results [14, 15], pectin dissolved at 6 wt% at pH 2.0 with R(Ca) = 0.2 yielded robust pectin hydrogels after 48 h. In these conditions both acid gelation and ionic gelation take place, the latter occurs as some of the carboxyl groups (~ 10 %) are deprotonated. The ionic gelation was necessary to prevent collapse during drying of xerogels and cryogels. Second, the comparison of the release properties of non-crosslinked (in the absence of Ca^{2+}) pectin hydrogels and aerogels will be performed.

Table 1 and Figure 2 show that the drying method has a marked influence on various properties of the pectin networks. For pectin cryogels, limited sample shrinkage is observed (10 - 13 vol %), which might originate from sample contraction upon immersion in liquid nitrogen to freeze water prior to sublimation. During freezing, ice crystals grow within the sample, compressing the walls of the pectin network and creating large pores. As a result, freeze-dried samples exhibit a very low density (0.07 g/cm^3), a high porosity (95 %) and a high pore volume (13 cm^3/g) as well as a rather damaged morphology with cracks and large macropores in the μm scale.

Table 1. Structural properties of pectin hydrogels, cryogels, aerogels and xerogels. All samples were prepared from 6 wt% pectin solution dissolved at pH 2.0 with R(Ca) = 0.2. Pore sizes were estimated from SEM images.

Matrix	**Hydrogel**	**Cryogel**	**Aerogel**	**Xerogel**
Bulk density (g/cm^3)	1.076 ± 0.009 ("wet" material)	0.073 ± 0.003 (dry material)	0.083 ± 0.005 (dry material)	1.057 ± 0.021 (dry material)
Volume shrinkage (%) Eq. 1	-	10 - 13	~ 30	> 90
Porosity (%) Eq. 2	-	95.1 ± 0.2	94.4 ± 0.3	29.5 ± 1.4
Pore volume (cm^3/g) Eq.3	-	13.03 ± 0.53	11.38 ± 0.75	0.28 ± 0.02
S_{BET} (m^2/g)	-	10 - 20	362 ± 14	Non-measurable
Network morphological aspect	-	Large macropores (0.5 - 5 µm in diameter)	Mesopores and small macropores (50 - 150 nm in diameter)	Dense network
Loading efficiency (%) Eq. 4	100	97	62	94

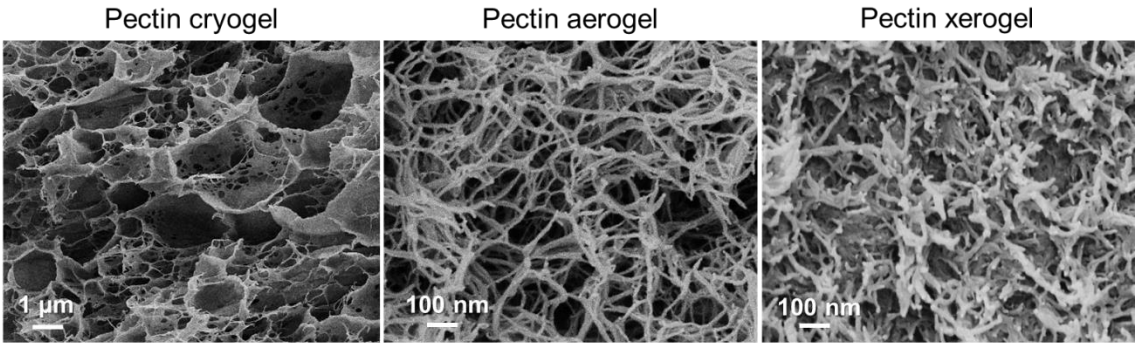

Figure 2.

SEM observations of a pectin cryogel, aerogel and xerogel. All samples were prepared from 6 wt% pectin solution dissolved at pH 2.0 with R(Ca) = 0.2.

Changing the drying method from freeze-drying (cryogels) to supercritical drying (aerogels) results in clear structural differences, most notably in terms of specific surface area and pore sizes. A supercritical fluid such as sc CO_2 has properties in between a liquid and a gas. As no meniscus is formed, capillary forces are avoided and samples dry almost without damage to the network structure. Some volume shrinkage (~ 30 vol%) occurs due to contraction during the water → ethanol exchange step and sc CO_2 drying, as observed frequently for aerogels [19]. After sc drying, low density aerogels are obtained (~ 0.080 – 0.085 g/cm^3) with a high porosity and pore volume, comparable to pectin cryogels. However, because the network remains almost intact, aerogels have much smaller pores, mainly mesopores and small macropores (50 to 150 nm in diameter). As a consequence, S_{BET} is much higher for aerogels (360 m^2/g compared to 10-20 m^2/g for cryogels). Evaporative drying (xerogels) performed under vacuum at 60 °C induces massive shrinkage (> 90 vol%). Structural collapse occurs due to important capillary forces, leading to materials with a high density (around 1 g/cm^3), a low porosity (~ 30%), a low pore volume (0.3 cm^3/g) and a compact

morphology after drying. Despite some porosity detected by SEM for pectin xerogels, the specific surface area was not measurable. It may be possible that some pores are closed.

Pectin hydrogels and cryogels loaded with theophylline (Figure 1) possess high (97-100 %) loading efficiencies. The pectin xerogel also exhibits a high loading efficiency (94 %), confirming that the impregnation time was sufficient to fully load the pectin alcogel. In contrast, the pectin aerogel shows a lower loading efficiency (~ 62%), which may originate from physical theophylline washout during sc CO_2 drying.

3.2 Theophylline release from pectin networks: influence of drying

The influence of the drying method on theophylline release kinetics was investigated by placing the pectin networks in SGF (pH 1.0) for 1 hour and subsequently in SIF (pH 6.8) to mimic the conditions in the gastro-intestinal tract. The evolution of theophylline release, matrix mass and matrix volume over time for pectin hydrogels, cryogels, aerogels and xerogels are presented in Figure 3.

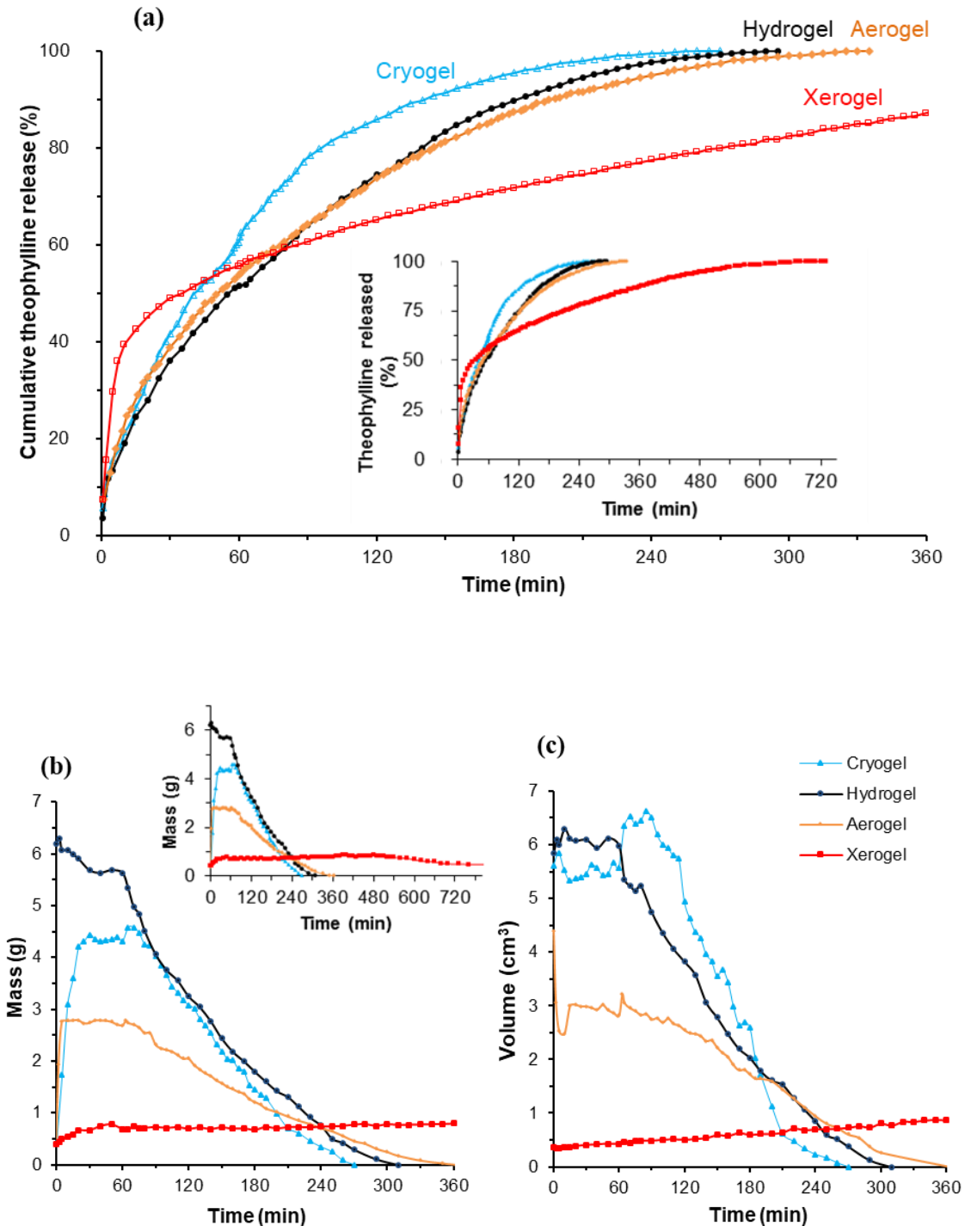

Figure 3.

Representative dependences of the cumulative theophylline release (a), matrix mass (b) and matrix volume (c) over time for pectin hydrogels, cryogels, aerogels and xerogels. All samples were prepared from 6 wt% pectin solution dissolved at pH 2.0 with R(Ca) = 0.2.

Hydrogels. The matrix mass and volume of the hydrogel remain constant in SGF medium (first hour) as the pectin chains are protonated and practically do not dissolve (Figures 3b and 3c). Upon change of the release medium from SGF to SIF (pH 6.8), ionization of the carboxylate groups of pectin takes place and the chains repel each other due to coulombic repulsion. As a result, the chains disentangle and start to dissolve as revealed by erosion until full dissolution after 290 min (Figures 3b and 3c). The matrix mass and volume evolution over time can be used to explain the kinetics of theophylline release (Figure 3a) from the pectin hydrogel, thereby also employing the Korsmeyer-Peppas and Peppas-Sahlin models [20, 21] which take into account diffusion and relaxation mechanisms:

$Q(t) = K_{KP} t^n$ (Korsmeyer-Peppas model, $Q(t) < 60$ %) (5)

where $Q(t)$ is cumulative release, t is time and n and K_{KP} are constants.

$$Q(t) = K_{\mathrm{F}} t^m + K_{\mathrm{R}} t^{2m} = F + R\,; \quad \frac{R}{F} = \frac{K_R}{K_F} t^m \ (Q(t) < 60\ \%) \qquad (6)$$

where K_F is diffusion constant, K_R is relaxation constant, m is Fickian diffusion exponent, R is relaxational and F Fickian contributions, respectively.

An n value of 0.54 is obtained after fitting the experimental data from Figure 3a for the first 60 % of drug release in the Korsmeyer-Peppas (eq.5) model with $R^2 > 0.99$ (Figure S1). This n value is typical for anomalous transport indicating that both solvent diffusion and polymer relaxation must be considered. As release takes largely place in SGF during the first 60 % of release (Figure 3), erosion is not yet significant. The Peppas-Sahlin model (eq. 6) can be used to estimate the relative contributions of the diffusion and relaxation mechanisms. The results presented in Figure S2 for the first 60% of release show that at the beginning of the release, diffusion prevails as drug release is mainly due to diffusion through the surface layers of the hydrogel. Over time, the contribution

of the diffusional mechanism decreases and polymer relaxation becomes important for the release of drug molecules that are located deeper in the matrix. Upon change from SGF to SIF, hydrogel erosion and dissolution become important, resulting in an increased mesh size of the polymer network, which in turn increases solvent velocity and drug transport through the matrix. Full theophylline release from the hydrogel occurs in 290 min (Figure 3a), slightly before the hydrogel fully dissolves (Figures 3b and 3c). This behavior is classical for polymer hydrogels used as drug carriers.

Cryogels. During the first 20 minutes of immersion in release medium (SGF, pH 1.0), the pectin cryogels exhibit a fast mass increase due to water uptake (Figure 3b), while their volume remains constant (Figure 3c). Following the change from SGF to SIF, the higher pH promotes ionization of pectin chains and the matrix immediately swells (Figure 3c). The cryogel subsequently dissolves, until full dissolution at t = 270 min. The fast release from the cryogels (Figure 3a) can be explained by their macroporous morphology (Figure 2), which facilitates solvent penetration and drug transport through the matrix. The higher velocity of solvent transport also follows from the Korsmeyer-Peppas *n* exponent value of 0.58 (Figure S1, first 60 % drug release, taking place entirely in SGF), which is slightly higher than the value for pectin hydrogels (0.54). The combination of fast solvent penetration into the low-density network with large pores likely promotes polymer relaxation, which is corroborated by the high relaxational constant K_R and high relative contribution of relaxation to the release according to the Peppas-Sahlin model (Figure S2). In SIF, rapid matrix erosion (Figures 3b and 3c) occurs, which further facilitates drug release until all is released at t = 270 min.

Aerogels. Similar to pectin cryogels, pectin aerogels quickly absorb release medium upon immersion, resulting in a fast mass increase (Figure 3b). The initial volume shrinkage of the aerogels likely results from the collapse of small pores due to capillary forces exerted by the fast

solvent penetration into the system (Figure 3c) [22]. Until the change of release medium, the aerogels exhibit a constant mass and volume thanks to the hydrogen bonding between pectin chains. In SIF the aerogels start to dissolve due to columbic repulsion between the ionized carboxylate groups, but the mass and volume loss occur slower compared to the pectin hydrogel and cryogel. Compared with pectin cryogels, aerogels have much smaller pores in the nanometric scale (Figure 2), which results in slower solvent penetration in the matrix and, as a consequence, slower matrix erosion (Figures 3b and 3c). Contrary to pectin hydrogels and cryogels, a dry core in pectin aerogels is maintained during the first hours of the release experiment, confirming slow solvent transport through the dry system (Figure 4).

Because of the hindered solvent penetration in aerogels, pectin chain relaxation is limited. This is also demonstrated by the lower Korsmeyer-Peppas exponent n = 0.49 (Figure S1) and Peppas-Sahlin relaxational constant K_R as well as the lower contribution of relaxation to the release (Figure S2) for the first 60 % release compared with hydrogels and cryogels. The contribution of diffusion is, however, relatively high for aerogels and the release profiles for pectin aerogels and hydrogels are rather similar until 60 % release. The slightly slower release of theophylline from aerogels compared to hydrogels is at later timepoints (full theophylline release in 330 min, Figure 3a) and may be due to the slower aerogel matrix erosion in SIF.

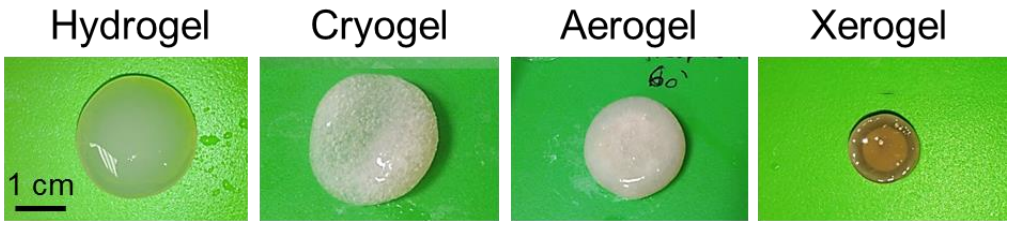

Figure 4.

Pictures of a pectin hydrogel, cryogel, aerogel and xerogel after immersion (37 °C) in simulated gastric fluid (SGF, pH 1.0) for one hour and subsequently in simulated intestinal fluid (SIF, pH 6.8) for another hour. All samples were prepared from 6 wt% pectin solution dissolved at pH 2.0 with R(Ca) = 0.2. The scale is the same for all pictures.

Xerogels. Pectin xerogels exhibit significant shrinkage during drying (~ 93-95%), which leads to a small sample volume (Figure 3c), a high density and a low porosity (Table 1). The compactness of the structure prevents both solvent penetration and matrix dissolution, which is confirmed by the maintenance of a dry core in the center of the matrix after 2 hours (Figure 4). Pectin xerogel samples keep their integrity during a long period of time ($t > 800$ min) and no matrix erosion takes place until 500 min of experiment (inset in Figure 3b). The burst release during the first 10 minutes may represent drug that was located on and near the surface. It is hypothesized that during the vacuum drying of the theophylline-loaded alcogels, the drug is partially transported towards the surface. Since no erosion takes place until 97% drug release, theophylline is released mainly by diffusion which is strongly perturbed by the presence of a dense network. The Korsmeyer-Peppas model (first 60 % drug release) affords an n exponent value of 0.23 (Figure S1). This n value indicates a deviation from Fick's law as $0.23 < 0.45$ (Case I Fickian diffusion), which may be due to the polydispersity of pore sizes, an overall heterogeneity within the material as well as the presence of closed pores [23]. When the pores of a polysaccharide-based material close during drying, they may not re-open during wetting, which is a phenomenon called hornification for cellulose. Peppas-Sahlin model was not applicable for the case of xerogels. The slow matrix erosion coupled with the slow drug diffusion through the highly dense network results in an extended release up to 10 hours (inset in Figure 3a).

3.3 Theophylline release from non-crosslinked pectin aerogel and hydrogel

Figure 3b shows that the kinetics of theophylline release from aerogel and hydrogel are very similar, with a slightly longer time of the complete theophylline release from aerogel, 340 vs 290 min, respectively. This was the case when pectin was crosslinked with calcium at R(Ca) = 0.2. In contrast, when pectin is not crosslinked, the difference in drug release behavior between pectin aerogels and hydrogels becomes significant, with complete release of theophylline in 300 and 150 minutes, respectively (Figure 5). In both cases, full theophylline release occurs just before complete matrix dissolution, but hydrogel dissolution takes place twice as fast. Without calcium, pectin hydrogels are soft and fragile as the chains are linked only by weak hydrogen bonds and hydrophobic interactions. The erosion of such hydrogels and drug release is much faster, especially in SIF, than from its crosslinked counterpart, recall Figure 3. When such a weak hydrogel is placed in a non-solvent and subsequently in sc CO_2 to make an aerogel, it shrinks significantly resulting in an aerogel with a density almost three times higher than its crosslinked counterpart: 0.215 vs 0.083 g/cm^3, respectively. The higher density is confirmed by the internal network morphology as shown in Figure 6, compare with the aerogel morphology in Figure 3. The reason for the different release behavior of non-crosslinked pectin hydrogel and aerogel is their very different network morphology despite the fact that the aerogel was made from the same precursor. A denser network is less prone to erosion as solvent penetration is slow due to the small pores, high tortuosity and thicker pore walls (Figure 6).

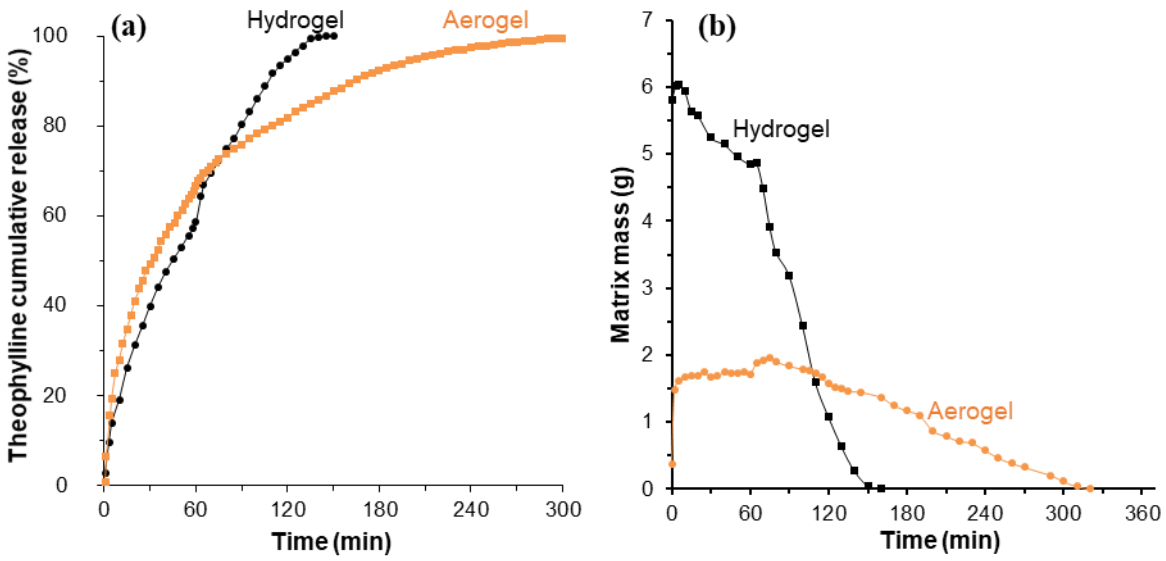

Figure 5.

Representative dependences of the cumulative theophylline release (a) and matrix mass (b) over time for pectin hydrogels and aerogels. All samples were prepared from 6 wt% pectin solution dissolved at pH 2.0 in the absence of calcium.

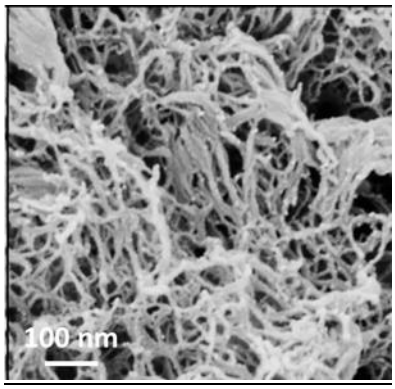

Figure 6.

Morphology of aerogel from 6 wt% pectin solution dissolved at pH 2.0 in the absence of calcium.

4. Conclusions

Pectin hydrogels were prepared and the influence of drying (freeze-drying, with supercritical CO_2 and evaporation under low vacuum) on material density, morphology and specific surface area was studied. Freeze-drying resulted in porous pectin with very low density (0.07 g/cm^3), micron-size pores, very high pore volume and low specific surface area (10-20 m^2/g); we assume that the morphology of pectin hydrogel is strongly distorted by ice crystals. After supercritical drying pectin was with low density (0.08 g/cm^3), meso- and small macropores, high pore volume and high specific surface area (360 m^2/g); this drying is probably the best way to reflect the morphology of hydrogels. Low vacuum evaporative drying resulted in pectin with low porosity and non-measurable surface area.

The kinetics of theophylline release from pectin hydrogel and the corresponding dry counterparts were investigated in simulated gastric fluid (for the first hour) followed by simulated intestinal fluid. In order to correlate the release kinetics with the mechanisms governing the release, sample mass and volume evolution were monitored. When pectin was crosslinked with calcium, the total release time followed the order cryogel < hydrogel < aerogel < xerogel. For cryogels, solvent penetration into the large pores of the low-density network is fast: diffusion of the drug out of the matrix is accompanied by polymer relaxation. The kinetics of theophylline release from hydrogel and aerogel based on calcium crosslinked pectin is similar, with a diffusion mechanism dominating the first 60 % of release. However, the total release time from aerogels is longer due to slower matrix erosion. For xerogels, the burst release occurs during the first 30-40 min most probably due to the dissolution of theophylline which is on and near the sample surface. Solvent uptake, matrix erosion and drug diffusion in xerogel are very slow; we hypothesise that this is partly due to the low and closed porosity of the network.

Opposite to the case of calcium crosslinked pectin, non-crosslinked hydrogel and aerogel show different release kinetics, especially in simulated intestinal fluid, with the hydrogel releasing theophylline twice quicker than the corresponding aerogel. Non-crosslinked hydrogel also dissolves much quicker than the crosslinked hydrogel as the chains are linked only by hydrogen bonds due to pectin acid gelation in the initial solution. Aerogel obtained from such a weak gel has a more than twice higher density and smaller pores than its non-crosslinked counterpart, which slow down drug diffusion and matrix erosion.

The results obtained show the versatility of pectin matrices whose release properties can be tuned by calcium crosslinking and drying mode.

Acknowledgements

We thank Cargill, France, for providing pectin, Pierre Ilbizian (PERSEE, Mines ParisTech, France) for supercritical drying, Laurent Schiatti De Monza (PERSEE, Mines ParisTech, France) for setting the automatic recording of theophylline release and Suzanne Jacomet (CEMEF, Mines ParisTech) for help with SEM imaging.

This research did not receive any specific grant from funding agencies in the public, commercial, or not-for-profit sectors.

Data availability:

The raw/processed data required to reproduce these findings cannot be shared at this time due to technical or time limitations.

References

[1] L.R. Adetunji, A. Adekunle, V. Orsat, V. Raghavan, Advances in the pectin production process using novel extraction techniques: A review, Food Hydrocolloids 62 (2017) 239-250.

[2] G.A. Martău, M. Mihai, D.C. Vodnar, The use of chitosan, alginate, and pectin in the biomedical and food sector - biocompatibility, bioadhesiveness, and biodegradability, Polymers 11 (2019) 1837.

[3] F. Munarin, M.C. Tanzi, P. Petrini, Advances in biomedical applications of pectin gels, Int. J. Biol. Macromol. 51 (2012) 681-689.

[4] B. Jurišić Dukovski, L. Mrak, K. Winnicka, M. Szekalska, M. Juretić, J. Filipović-Grčić, I. Pepić, J. Lovrić, A. Hafner, Spray-dried nanoparticle-loaded pectin microspheres for dexamethasone nasal delivery, Drying Technol. 37 (2019) 1915-1925.

[5] V. Kulikouskaya, A. Kraskouski, K. Hileuskaya, A. Zhura, S. Tratsyak, V. Agabekov, Fabrication and characterization of pectin-based three-dimensional porous scaffolds suitable for treatment of peritoneal adhesions, J. Biomed. Mater. Res., Part A 107 (2019) 1814-1823.

[6] K. Ganesan, T. Budtova, L. Ratke, P. Gurikov, V. Baudron, I. Preibisch, P. Niemeyer, I. Smirnova, B. Milow, Review on the production of polysaccharide aerogel particles, Materials 11 (2018) 2144.

[7] N. Buchtova, T. Budtova, Cellulose aero-, cryo-and xerogels: towards understanding of morphology control, Cellulose 23 (2016) 2585-2595.

[8] M.V. Konovalova, P.A. Markov, E.A. Durnev, D.V. Kurek, S.V. Popov, V.P. Varlamov, Preparation and biocompatibility evaluation of pectin and chitosan cryogels for biomedical application, J. Biomed. Mater. Res., Part A 105 (2017) 547-556.

[9] D. Demir, S. Ceylan, D. Göktürk, N. Bölgen, Extraction of pectin from albedo of lemon peels for preparation of tissue engineering scaffolds, Polym. Bull. (2020) 1-16.

[10] Y. Mata, M. Blázquez, A. Ballester, F. González, J. Muñoz, Studies on sorption, desorption, regeneration and reuse of sugar-beet pectin gels for heavy metal removal, J. Hazard. Mater. 178 (2010) 243-248.

[11] Y. Mata, M. Blázquez, A. Ballester, F. González, J. Muñoz, Sugar-beet pulp pectin gels as biosorbent for heavy metals: preparation and determination of biosorption and desorption characteristics, Chem. Eng. J. 150 (2009) 289-301.

[12] F. De Cicco, P. Russo, E. Reverchon, C.A. García-González, R.P. Aquino, P. Del Gaudio, Prilling and supercritical drying: A successful duo to produce core-shell polysaccharide aerogel beads for wound healing, Carbohydr. Polym. 147 (2016) 482-489.

[13] C.A. García-González, M. Jin, J. Gerth, C. Alvarez-Lorenzo, I. Smirnova, Polysaccharide-based aerogel microspheres for oral drug delivery, Carbohydr. Polym. 117 (2015) 797-806.

[14] S. Groult, T. Budtova, Tuning structure and properties of pectin aerogels, Eur. Polym. J. 108 (2018) 250-261.

[15] S. Groult, T. Budtova, Thermal conductivity/structure correlations in thermal super-insulating pectin aerogels, Carbohydr. Polym. 196 (2018) 73-81.

[16] G. Tkalec, Ž. Knez, Z. Novak, PH sensitive mesoporous materials for immediate or controlled release of NSAID, Microporous Mesoporous Mater. 224 (2016) 190-200.

[17] G. Horvat G, M. Pantić, Ž. Knez, Z. Novak, Encapsulation and drug release of poorly water soluble nifedipine from bio-carriers, J. Non-Cryst. Solids 481 (2018) 486-493.

[18] I. Braccini, S. Pérez, Molecular basis of Ca2+-induced gelation in alginates and pectins: the egg-box model revisited, Biomacromolecules 2 (2001) 1089-1096.

[19] C.A. García-González, M. Alnaief, I. Smirnova, Polysaccharide-based aerogels - Promising biodegradable carriers for drug delivery systems, Carbohydr. Polym. 86 (2011) 1425-1438.

[20] P.L. Ritger, N.A. Peppas, A simple equation for description of solute release II. Fickian and anomalous release from swellable devices, J. Controlled Release 5 (1987) 37-42.

[21] R.W. Korsmeyer, R. Gurny, E. Doelker, P. Buri, N.A. Peppas, Mechanisms of solute release from porous hydrophilic polymers, Int. J. Pharm. 15 (1983) 25-35.

[22] M.A. Marin, R.R. Mallepally, M.A. McHugh, Silk fibroin aerogels for drug delivery applications, J. Supercrit. Fluids 91 (2014) 84-89.

[23] G. Horvat, K. Xhanari, M. Finšgar, L. Gradišnik, U. Maver, Ž. Knez, Z. Novak, Novel ethanol-induced pectin–xanthan aerogel coatings for orthopedic applications, Carbohydr. Polym. 166 (2017) 365-376.